# Realization of a two-dimensional Ising system: Deuterium physisorbed on krypton-preplated graphite

Horst Wiechert and Klaus-Dieter Kortmann
*Institut für Physik, Johannes Gutenberg-Universität, Staudingerweg 7, D-55099 Mainz, Germany*

Norbert Stüßer
*BENSC, Hahn-Meitner-Institut, Glienicker Strasse 100, D-14109 Berlin-Wannsee, Germany*
(Received 28 January 2004; revised manuscript received 22 June 2004; published 15 September 2004)

Volumetric adsorption isotherm, calorimetric, and neutron diffraction measurements were used to characterize the quantum system $D_2$ coadsorbed on graphite preplated by a monolayer of Kr. From the results obtained by these methods a detailed phase diagram of the complete submonolayer coverage range up to the initial stages of bilayer formation could be constructed. The dominant feature of the phase diagram is a commensurate $(1\times1)\left[\frac{1}{2}\right]$ structure, which was determined by neutron diffraction. Three phase transitions of this phase were studied: The order-disorder transition at the critical point which, according to the influence of the corrugation potential, occurs at a relatively high temperature ($T_c$=25.68 K), the order-disorder transition at the tricritical point ($T_{TC}$=17.88 K), and the commensurate-incommensurate (C-IC) transition at $D_2$ fillings above $1.2\times\sqrt{3}$ monolayers. All these measurements gave convincing evidence that the system $D_2$/Kr/graphite can be regarded as realization of a two-dimensional (2D) Ising system. Critical exponents near the phase transitions were determined and good agreement with the theory obtained. Of particular interest was the investigation of the C-IC transition, which for a 2D Ising system could be studied. At this transition, the existence of a reentrant fluid was detected, which squeezes in between the *C* and IC phases down to at least 1.5 K, which is the lowest temperature to which a liquidlike phase of $D_2$ has ever been found. This observation confirms the Kosterlitz-Thouless criterion and the theory of the C-IC transition.

DOI: 10.1103/PhysRevB.70.125410 PACS number(s): 61.12.−q, 79.60.Dp, 64.60.Cn, 64.70.Rh

## I. INTRODUCTION

Physisorbed systems on graphite have proven to be fertile grounds for the realizations of ideas of statistical thermodynamics. Prominent examples are the light quantum gases $^3$He and $^4$He (Refs. 1–3) and the isotopes of molecular hydrogen ($H_2$, HD, and $D_2$)[4,5] adsorbed on the (001) basal planes of graphite. The properties of the hydrogen isotopomers are described in detail in a recent review article.[6] The five quantum systems have in common that they form a commensurate (*C*) $(\sqrt{3}\times\sqrt{3})R30°$ phase at submonolayer coverages and low temperatures due to the strong influence of quantum zero-point motions, which give rise to lateral repulsive interactions between the molecules and push them into the troughs of the graphite potential. For instance, for $D_2$ on graphite the well-known $\sqrt{3}$ phase is schematically illustrated in Fig. 1(a). The honeycomb network of carbon rings shows the basal plane of the graphite surface and the light gray disks—drawn with their hard-core Lennard-Jones diameters to scale—represent the adsorbed deuterium molecules in their ground states. The structure is threefold degenerate and can be realized on three energetically equivalent sublattices of adsorption sites in the centers of the carbon rings *A*, *B*, and *C* classifying the adsorbate as a three-state Potts system, one of the elementary models of statistical thermodynamics.[7] Usually the number of equivalent sublattices of adsorption sites is denoted by $p$ (i.e., $p=3$ for the three-state Potts system).

The main motivation of the present project was to realize a two-dimensional (2D) Ising system in physisorbed matter and to investigate as completely as possible its phases and phase transitions. As Vilches and co-workers[8] have convincingly demonstrated by calorimetric measurements, one possibility to build up such a system is to preplate graphite by a complete commensurate $(\sqrt{3}\times\sqrt{3})R30°$ monolayer of krypton and to coadsorbe $^4$He atoms on top of this layer. At about the same time Schick *et al.*,[9–12] classifying the continuous order-disorder transitions of adsorbed systems on the basis of the Landau theory, predicted that a transition of a $(1\times1)$ superlattice structure on a honeycomb array of adsorption sites will fall into the universality class of the 2D Ising model. Such a dramatic change from three-state Potts to Ising behavior can be provided by a Kr spacer layer, which modifies the symmetry of the array of adsorption sites from a triangular lattice on bare graphite to a honeycomb lattice. Figure 1(b) illustrates schematically the real situation, which we tried to attain in our experiments: $D_2$ adsorbed on Kr preplated graphite. As concluded from diffraction experiments[13,14] the $D_2$ layer compresses the Kr layer to a structure incommensurate to the substrate. Due to the size of the $D_2$ molecules, there are only two energetically equivalent possibilities to form an equilaterally spaced triangular adsorbate lattice on the Kr spacer layer, which is called a $(1\times1)\times\left[\frac{1}{2}\right]$ structure.[8] This means that this structure has the same nearest-neighbor spacing as Kr, but only half of the available adsorption sites are occupied. This structure has two ground states (*A* and *B*), i.e., it is expected to belong to the 2D Ising universality class ($p=2$).

In the present paper we shall study this system by using adsorption isotherm, heat capacity and neutron-diffraction measurements. While a few preliminary results have already

 

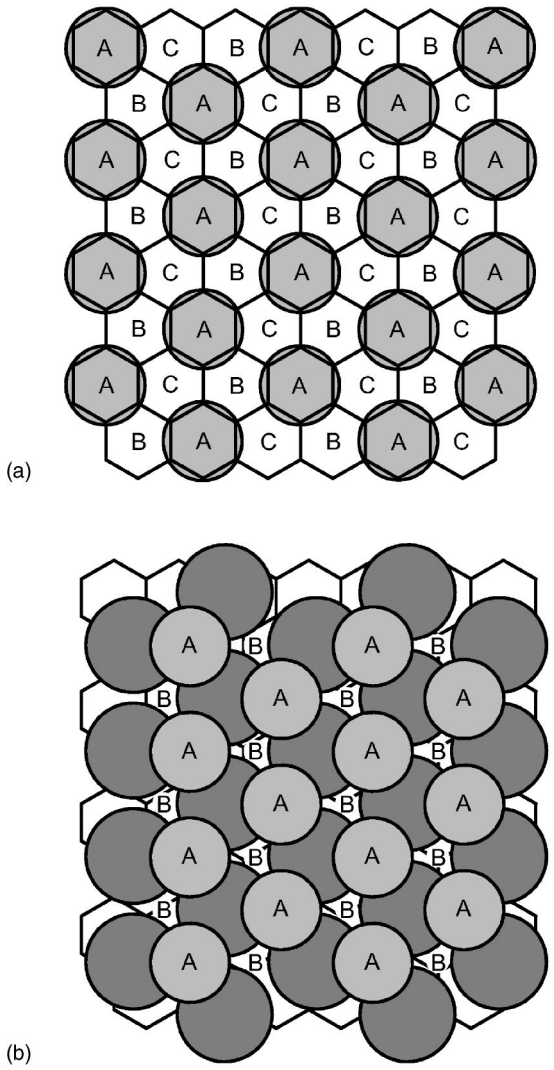


FIG. 1. (a) Schematic representation of the structure of the commensurate $(\sqrt{3}\times\sqrt{3})R30°$ phase of $D_2$ molecules adsorbed on the graphite basal plane which is indicated by the honeycomb lattice of carbon rings. The $D_2$ molecules (light gray disks) are drawn with their hard-core Lennard-Jones diameters. The structure is threefold degenerate and can be realized on three energetically equivalent sublattices of adsorption sites A, B, and C ($p=3$) which classifies the adsorbate as a three-state Potts system. (b) Structure of the commensurate $(1\times1)\left[\frac{1}{2}\right]$ phase of $D_2$ (light gray disks) adsorbed on graphite preplated by an incommensurate monolayer of Kr (dark gray disks) (Ref. 14). $D_2$ molecules and Kr atoms are shown with their hard-core Lennard-Jones diameters. Because of the two subsets of adsorption sites (A and B, $p=2$), this system should belong to the 2D Ising universality class.

been published previously,[14,15] this contribution will give a more detailed account of our experiments, which are conducted to explore all properties of a 2D Ising system and characterize them. In order to achieve this aim, we have chosen the system $D_2$ on Kr plated graphite as mentioned above. $D_2$ has a coherent neutron-scattering cross section, which is about a factor of 17 larger than that of $^4$He.[6] This advantage enables in addition to thermodynamic studies, also structural investigations by using neutron diffraction.

The paper is organized as follows. Section II describes some experimental aspects. In Sec. III, the sample will be characterized by using adsorption isotherm measurements. In Sec. IV we present results of heat capacity measurements, show calculations of entropy, and map out the phase diagram of $D_2$ on Kr preplated graphite up to the coverage region of the compressed monolayer. Neutron diffraction results, which corroborate the thermodynamic data, will be given in Sec. V. Section VI is devoted to the characterization of the phase transitions found at the critical and the tricritical point. We were able to determine the critical exponent of a 2D Ising system in the neighborhood of the tricritical point. The investigation of the commensurate-incommensurate transition provides convincing evidence for the prediction of Coppersmith *et al.*[16,17] that it is a melting transition and fulfills the Kosterlitz-Thouless criterion.[18,19] Section VII concludes the paper with a discussion and a summary of our results.

## II. EXPERIMENTAL ASPECTS

The thermodynamic studies of this work included volumetric adsorption isotherm and heat capacity measurements. The heat capacity data were obtained by employing the conventional quasiadiabatic heat-pulse technique (Nernst-Eucken calorimetry).[20] The calorimeter was a thin-walled cylindrical copper cell (diameter 30 mm, height 60 mm, wall thickness 0.3 mm). A piece of graphite Foam (exfoliated graphite, product of Union Carbide Corp.) with a total surface area of 74.96 $m^2$ (specific surface 24.74 $m^2/g$) was pressure fitted into the cell. This substrate can be regarded as a uniform powder consisting of single crystal flakes with a lateral extent of about 900 Å (coherence length).[21] Further details of the experimental method and substrate preparation are given in Ref. 20 and of the properties of different substrates and surface calibration in Refs. 6 and 22.

The neutron diffraction experiments were performed on the focusing diffractometer E6 (wavelength 2.38 Å) at the Hahn-Meitner-Institute (BENSC) in Berlin, Germany. As opposed to a conventional diffractometer, the focusing diffractometer employs a horizontally and vertically bent monochromator in combination with a vertical slit placed in the incoming beam of the monochromator. The neutron flux at the sample position was about $5\times10^6$ n/($cm^2$ s). The diffractometer was used in a standard configuration with an in-pile collimator of 20′ to reduce background scattering. The instrument was equipped with a multicounter with 200 channels of 0.1° width covering an angular range of 20°. For the neutron diffraction experiments, a stack of exfoliated graphite sheets (Papyex, trademark of Le Carbone-Lorraine) was used as the substrate. This material consists of graphite flakes with a characteristic length of step-free atomically flat basal surfaces of about 250 Å and with a mosaic spread of ±15°.[21] The sheets were closely packed into a cylindrical Al cell (diameter 20 mm, height 70 mm) and oriented parallel to the neutron-scattering plane. Compared to the graphite Foam sample used in the heat capacity measurements, the Papyex sample has the advantage of a larger total surface (381.85 $m^2$) which leads to a better counting statistics at the moderate measuring rates of the neutron diffraction experiments.

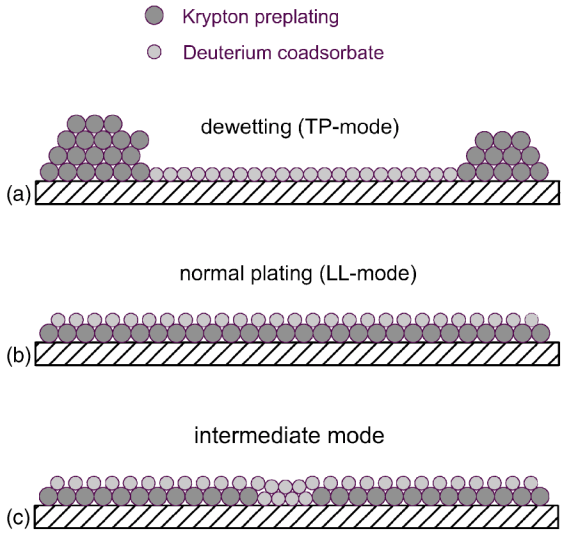


FIG. 2. Growth modes of $D_2$ on Kr preplated graphite. (a) The two-phase (TP) mode. The Kr plating (dark gray particles) is partially displaced by the $D_2$ molecules (light gray particles) and forms multilayers or 3D clusters on confined regions of the substrate (Ref. 23). (b) The normal layer-on-layer (LL) mode. The Kr layer is preserved and a $D_2$ monolayer forms on top of the Kr spacer layer (Ref. 23). (c) Intermediate mode: Layer-on-layer (LL) growth mode with $D_2$ islands being squeezed into the Kr layer. The penetration of the $D_2$ molecules results in a spreading pressure by which the Kr layer is compressed. The x-ray and neutron diffraction measurements (Refs. 13 and 14, and Sec. V) clearly reveal this type of growth mode.

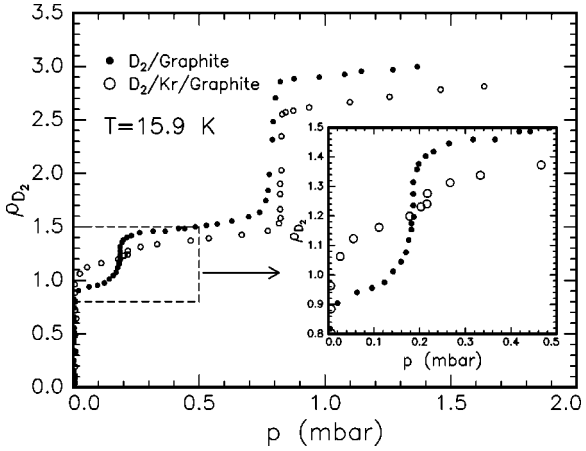


FIG. 3. Comparison of adsorption isotherms of $D_2$ on bare graphite (●) and on Kr plated graphite (○) at $T=15.9$ K. The Kr plating is 1 ML. The $D_2$ filling $\rho_{D_2}$ in units of a perfect $(\sqrt{3}\times\sqrt{3})R30°$ phase (one molecule per area of three graphite hexagons) is plotted vs the equilibrium vapor pressure. The stepwise isotherm behavior points to a layer-on-layer (LL) type of growth mode. The inset shows a magnified view of the C-IC transition region for both systems. The small step in the adsorption isotherm of $D_2$/Kr/graphite indicates that the C-IC transition also occurs, but takes place in a much smaller coverage range than that of $D_2$/graphite.

As adsorbates, $D_2$ gas (99.7% pure) and Kr with a nominal purity of 99.99% have been used. No special precaution has been taken to convert $D_2$ into the ground state (ortho-$D_2$), because we did not expect any orientational ordering effects on the observed phases in the temperature range above 1.5 K investigated in this work.[6] Even for time periods of more than a month for some experiments, the data were always reproducible. The coverages or fillings of the adsorbates were determined by measuring adsorption isotherms with $N_2$ at 77 K. A substep occurring in such an isotherm is associated with the transition between a fluid phase and a solid phase in registry with the graphite substrate. The upper end of the substep is considered to correspond to the completion of the perfect $\sqrt{3}$ phase, is defined as $\rho=1$ [one monolayer (ML)], and was taken as reference point for our coverage calibrations.

Most of the data presented in this paper were taken by preplating the graphite substrate by a complete $\sqrt{3}$ monolayer of Kr. For consistency checks, in a few cases we also choose a Kr-preplating of 1.15 ML, but found no substantial differences.

## III. COADSORBATE CHARACTERIZATION BY ADSORPTION ISOTHERMS

The first step to explore an unknown coadsorbate is to measure an adsorption isotherm. Following Asada *et al.*,[23] in principle there may occur two different growth modes of a film due to the different adsorption energies of the coadsorbed species as depicted schematically in Fig. 2. One of them [Fig. 2(a)] is the two-phase (TP) mode, in which the $D_2$ molecules (light gray particles) squeeze themselves into the preadsorbed Kr layer (dark gray particles) and partially displace it. The Kr atoms then form multilayers or 3D clusters in limited surface regions. The second mode is the normal plating or layer-on-layer (LL) mode, where the Kr plating is preserved [Fig. 2(b)] and a $D_2$ layer forms on top of the Kr layer. Ignoring entropy and mixing effects of the two different types of atoms or molecules,[24] estimations based on simple energetic considerations according to the model proposed by Asada *et al.*[23] lead to the result that the total adsorption energy for the LL mode is higher than that of the TP mode. Thus, it is to be expected that $D_2$ on Kr/graphite will grow in the LL mode rather than in the TP mode. The real situation, however, is an intermediate state between these two growth modes, which is illustrated in Fig. 2(c). It will be discussed in Sec. V.

In order to distinguish experimentally between the first two modes, we carried out adsorption isotherm measurements. In Fig. 3, an adsorption isotherm of $D_2$ on bare graphite is compared to that of $D_2$ on graphite preplated by 1 ML of Kr at $T=15.9$ K. The $D_2$ filling is plotted versus the equilibrium vapor pressure $p$. Several vertical steps occur which reveal that both systems grow in the layer-on-layer (LL) mode at least up to the formation of the third layer. The vertical risers mark regions of constant chemical potential and thus correspond to phase transition regions of the adsorbed systems. The pressure differences, where the steps appear, reflect differences in the holding potential of the two systems. The inset of the figure shows a magnified view of the commensurate-incommensurate transition region (for

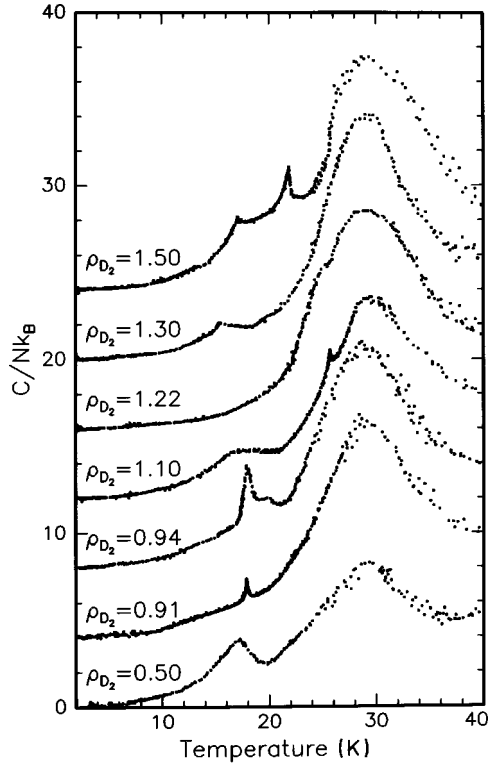


FIG. 4. Heat capacity scans ($N$=number of adsorbed particles, $k_B$=Boltzmann constant) at various $D_2$ fillings on Kr preplated graphite. The background contributions of the substrate and the sample cell have been subtracted. Except for the data set at the lowest $D_2$ filling, for clearness in representation all others have been shifted along the ordinate by adding a constant offset. The anomalies indicate phase transitions in the $D_2$ film except for the broad peaks around 29 K which are caused by desorption of $D_2$ molecules.

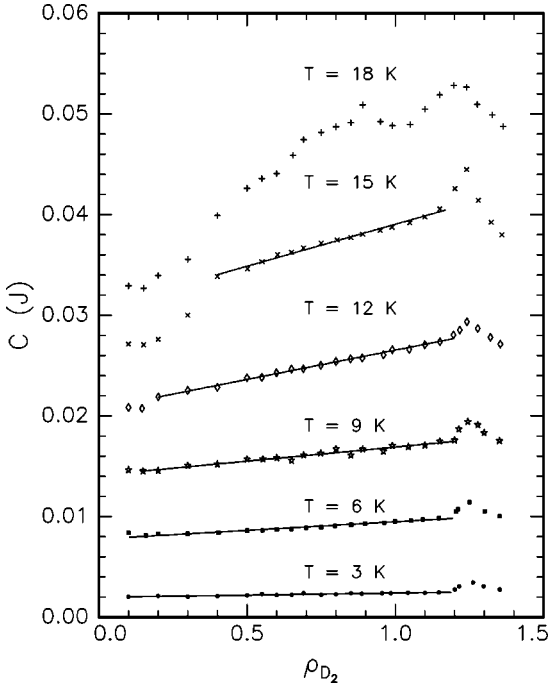


FIG. 5. Heat capacity isotherms at various temperatures between 3 and 18 K. Linear coverage regions reveal the likely existence of a coexistence region between 2D solid [commensurate $(1\times1)[\frac{1}{2}]$ phase] and 2D gas. The end points of the straight lines correspond to phase transitions. For clearness of representation, offsets have been added to the curves.

comparison with $D_2$/graphite see Refs. 4–6 and 25). The small step at $p=0.22$ mbar observed for $D_2$/Kr/graphite leads one to assume that this transition also might occur, but takes place in a much reduced coverage range.

## IV. HEAT CAPACITY RESULTS AND PHASE DIAGRAM

Being now relatively confident that the coadsorbate behaves in the desired manner, we carried out a series of specific heat measurements. They were made at about 60 $D_2$ fillings in the range $0\leqslant\rho_{D_2}\leqslant2$ to map out the boundaries of the phase diagram in detail. Figure 4 shows a few representative heat capacity scans versus temperature at $D_2$ fillings between 0.5 and 1.5 $\sqrt{3}$ monolayers (ML). The Kr preplating was again 1 ML. Note that all $D_2$ fillings given in this work are low-temperature values before desorption effects set in. The heat capacity is given in reduced units with $N$ the number of $D_2$ molecules dosed into the sample cell and $k_B$ the Boltzmann constant. The background of the calorimeter and the Kr layer has been subtracted from the data. The dominant feature of the scans is a large and broad peak occurring at a temperature centered at about 29 K for all $D_2$ fillings. From separate vapor pressure measurements as a function of temperature[26] we found out that it is caused by desorption of the $D_2$ layer.

In order to analyze this peak, we applied a simple model developed by Ebey *et al.*[27] It is based on the assumption that the adsorbate can be regarded as a 2D ideal gas bound with constant energy per particle to the surface before desorbing into the 3D gas. Even if the assumption of a 2D ideal gas in case of $D_2$ is a very crude approximation, from the desorption peak temperature we estimated a binding energy of the $D_2$ molecules to the Kr spacer layer on graphite of roughly −175 K. This value is by about a factor of three smaller than that of $D_2$ on bare graphite [−517.6 K (Ref. 28).]

The heat capacity peaks signaling the phase transitions of the $D_2$ layer are smaller and appear at lower temperatures than the desorption peak (Fig. 4). Starting at $\rho_{D_2}=0.50$, they become more pronounced with increasing $D_2$ filling and split into a double peak above $\rho_{D_2}=0.91$. The high-temperature peak shifts rapidly with growing coverage to 25.68 K at $\rho_{D_2}=1.10$, where it resides on the low-temperature wing of the desorption peak. The low-temperature peak broadens, decreases in height and moves slightly to lower temperatures. In a small coverage range around $\rho_{D_2}=1.22$ almost every feature disappeared and at $\rho_{D_2}=1.30$, a new anomaly arises, which separates into two peaks at higher coverages ($\rho_{D_2}=1.50$).

From the heat capacity data, we constructed heat capacity isotherms, which are presented in Fig. 5 by plotting $C$ versus $\rho_{D_2}$ at fixed temperatures between 3 and 18 K. Several linear regions are discernible which shrink in coverage range with

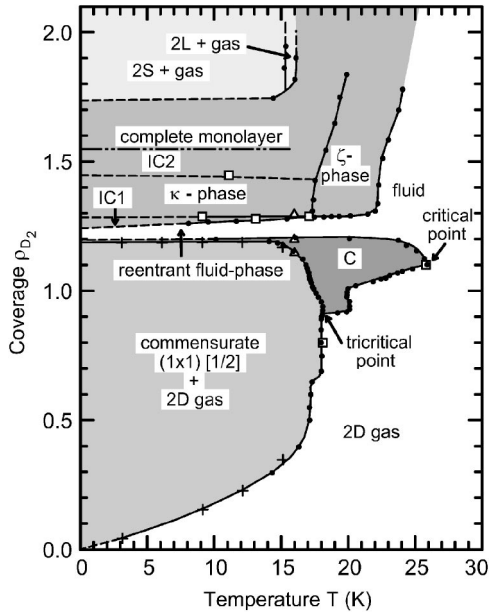


FIG. 6. Proposed phase diagram of $D_2$ adsorbed on graphite preplated by a monolayer of Kr equivalent to a coverage of $\rho_{Kr}=1$. The phase diagram was constructed from heat capacity data (solid circles), end points of linear regions of heat capacity isotherms (crosses), adsorption isotherm data (open triangles), and phase boundaries determined by neutron diffraction (open squares). C: Commensurate $(1\times1)\left[\frac{1}{2}\right]$ phase, IC1, IC2: incommensurate phases with different lattice constants, $\kappa$, $\zeta$ phase: incommensurate phases of unknown structure, 2S: second layer solid, 2L: second layer liquid. Most of the phases were identified by neutron diffraction. Solid lines indicate phase boundaries inferred from experimental data, dashed lines are suspected phase boundaries, and the double-dotted-dashed line marks the completion of the $D_2$ monolayer. In a small coverage range at the C-IC transition a reentrant fluid phase squeezes in between the C and the IC phases as expected from the theory (Refs. 16 and 17) for a 2D Ising system. $\rho_{D_2}=1$ is defined as filling in units of number of molecules per area of three graphite hexagons.

increasing temperature. According to Dash *et al.*,[29,30] these linear regions indicate a two-phase coexistence region which is also supported by the adsorption isotherm at 15.9 K in Fig. 3. The end points of the linear regions mark boundaries of the phase diagram.

With the information gained from all these measurements, we mapped out the phase diagram of $D_2$ adsorbed on graphite preplated by a complete monolayer of Kr ($\rho_{Kr}=1$), which is shown in Fig. 6. It contains data from locations of heat capacity peaks (solid circles, Fig. 4), end points of linear regions of heat capacity isotherms (crosses, Fig. 5), data from an adsorption isotherm (open triangles, Fig. 3), and phase boundaries determined from neutron diffraction measurements (open squares), which will be described in Sec. V. Where data were available from the various methods employed, they agree very well with each other. Phase boundaries at higher temperatures and coverages are corrected for desorption effects as determined by vapor-pressure measurements.

The structures of most of the phases found were identified by neutron diffraction (see Sec. V). From linear regions in heat capacity isotherms and the neutron diffraction data, it was inferred that there is a broad coexistence region between a commensurate $(1\times1)\left[\frac{1}{2}\right]$ solid phase and a 2D gas at $D_2$ fillings below $\rho_{D_2}=1.18$ and at low temperatures. The shapes of the phase boundaries suggest that this region ends at the tricritical point ($T_{TC}=17.88\pm0.06$ K, $\rho_{D_2}=0.91\pm0.01$). Probably due to thermal contributions, the region of the pure commensurate ($C$) $(1\times1)\left[\frac{1}{2}\right]$ phase is restricted to high temperatures, except for a very narrow strip extending down to low temperatures at $D_2$ fillings between 1.19 and 1.20. The $C$ phase is expected to contain vacancies at lower ($\rho_{D_2}<1.1$) and interstitials at higher coverages ($\rho_{D_2}>1.1$). It terminates at the critical point at $T_c=25.68\pm0.05$ K and $\rho_{D_2}=1.10\pm0.01$. Note that this coverage is about 10% higher than that of the ideal coverage for a $\sqrt{3}$ structure ($\rho=1$), because this fraction of $D_2$ molecules intrudes in the Kr spacer layer and compresses it to an incommensurate phase as we will see in Sec. V. The critical temperature is anomalously high. For comparison, the critical temperature of the order-disorder transition of the commensurate $(\sqrt{3}\times\sqrt{3})R30°$ phase of $D_2$ on bare graphite is $T_c=18.1$ K.[4,6,25] Since the binding energy of $D_2$ on Kr/graphite is a factor of three smaller than that on bare graphite as estimated from the desorption peaks, we conclude that a greater amplitude of potential corrugation might be responsible for this effect. An analogous observation was made previously for $^4$He on Ar- or Kr-plated graphite.[8,31,32] In order to understand this effect more quantitatively, for instance, computer simulations as performed for the hydrogen isotopes on bare graphite[33–36] would be very helpful.

At $D_2$ fillings above 1.25 ML at low temperature incommensurate solid phases are formed. The monolayer is complete at $\rho_{D_2}=1.55$ beyond which the second layer is built up. At still higher coverages, above $\approx$1.72 ML, it exhibits features of a 2D van der Waals system with coexistence regions between solid and gas (2S+gas) and liquid and gas (2L+gas), which is reminiscent of the phase diagram of the second layer of $D_2$ on graphite.[6,37] 2S and 2L are abbreviations of second layer solid and second layer liquid, respectively.

An unusual feature is the gap in the phase diagram for $1.20<\rho_{D_2}<1.25$ at the commensurate-incommensurate (C-IC) transition. In this coverage range, no heat capacity anomalies could be found (see Fig. 4). A clue to the nature of the $D_2$ film in this range of the phase diagram is provided by entropy data which were obtained from the heat capacity $C(T)$ according to the relation

$$S(T)=\int_0^T \frac{C(T')}{T'}dT'. \tag{1}$$

Since heat capacity data below 1.5 K were not measured, we extrapolated the data to $T=0$ K by using the 2D Debye law ($C\sim T^2$). In Fig. 7, the results including the extrapolated values at various coverages between $1.15<\rho_{D_2}<1.29$ are shown. It is evident that the data in the range of the gap of the phase diagram ($\rho_{D_2}=1.21$, 1.22, and 1.24) exhibit enhanced values at low temperatures compared to those at

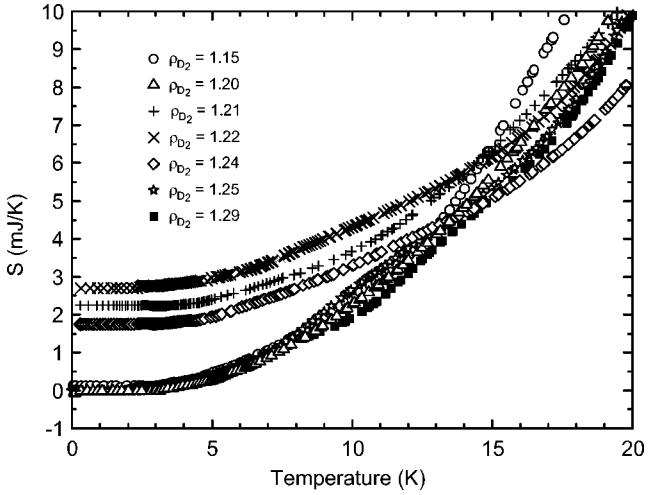


FIG. 7. Entropy $S$ calculated from heat capacity data according to Eq. (1) versus temperature at selected $D_2$ fillings $\rho_{D_2}$. The data clearly reveal enhanced entropy in the coverage region $1.20 < \rho_{D_2} < 1.25$ at low temperatures pointing to a high degree of disorder. Data below 1.5 K (except those at coverages between 1.20 and 1.25 ML, which are speculative) show extrapolated values calculated by assuming a 2D Debye law.

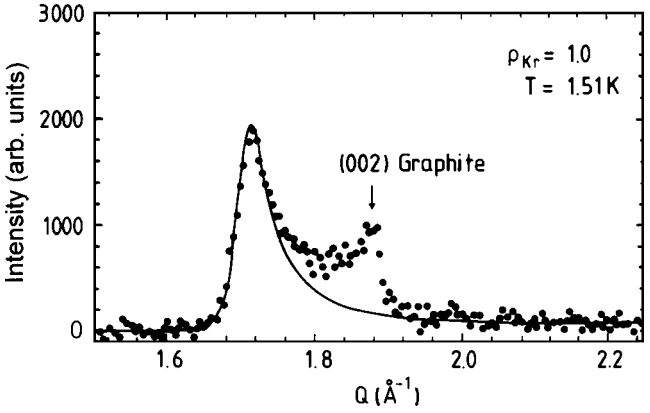


FIG. 8. Neutron diffractogram of Kr adsorbed on bare graphite at $T = 1.51$ K and $\rho_{Kr} = 1$. The Kr layer adopts a commensurate $(\sqrt{3} \times \sqrt{3})$ $R30°$ phase. Solid line: Fit to the Bragg peak by a powder-averaged Lorentzian-squared line shape convoluted with the instrumental resolution (Ref. 39).

higher or lower coverages. This indicates that the $D_2$ film in the gap is in a state of higher disorder. Further evidence for this observation will also be provided by neutron diffraction (see Sec. V). Because of these findings (and due to the analogy with $D_2$ on graphite[4–6,25]) we tentatively attributed this region to the existence of a reentrant fluid (domain-wall fluid phase). Probably this phase possesses residual entropy down to very low temperatures (as tentatively indicated in the figure by the extrapolated entropy data), much lower than 1.5 K, the lowest temperature achieved in our experiments. This is the lowest temperature to which a translationally disordered phase of $D_2$ could ever be observed in nature.

## V. NEUTRON DIFFRACTION RESULTS

In order to explore the nature of the various phases found in the heat capacity measurements, we carried out neutron diffraction measurements. To be able to discriminate the contribution of the Kr spacer layer, we first recorded a neutron-diffraction pattern of a complete monolayer of Kr ($\rho_{Kr} = 1$) adsorbed on graphite at $T = 1.51$ K which is depicted in Fig. 8. The background scattering from the unloaded sample cell has been subtracted from the data, which has also been done for all other diffractograms displayed in this paper. The subtracted substrate signal has not been scaled to account for Kr or $D_2$ absorption. The residual peak at wave vector $Q = 1.873$ Å$^{-1}$ is due to some interference effect between the adlayer and the substrate in combination with imperfect subtraction of the strong (002) graphite reflection, which partially may result from ignoring absorption by the Kr and $D_2$ layers. The data clearly exhibit a Bragg peak from the Kr layer. From its position at $Q = 1.703$ Å$^{-1}$ we infer that the Kr layer at $\rho_{Kr} = 1$ adopts a $(\sqrt{3} \times \sqrt{3})R30°$ structure. The peak was fitted by an asymmetric Warren[38] profile (solid line) characteristic of a 2D powder. The line shape results from the random orientations of the 2D monolayer patches adsorbed on graphite crystallites by assuming the percentages of isotropic (70%) and preferred (30%) orientation with a vertical mosaic spread of about 30° of the basal planes. (For properties of different graphite substrates, see, e.g., Refs. 6 and 21.) Empirically we found that an intrinsic Lorentzian-squared line shape, which was powder averaged and convoluted with the instrumental resolution function,[39] provides the best fits to data obtained by our relatively low-resolution neutron-diffraction measurements. We used the line shape of Ref. 39 to describe the Bragg peaks of all the diffraction measurements in this work. From the fit shown in Fig. 8, a coherence length of about 250 Å was obtained, which corresponds to the typical size of the crystallites of the Papyex graphite substrate employed.[6,21]

Figure 9 demonstrates what happens when $D_2$ is coadsorbed at $T = 1.57$ K. The first scan at the bottom again refers to pure Kr. Admitting a small dose of $D_2$ (0.049 ML) leads to a splitting of the peak. The low-$Q$ component of the peak remains at the commensurate position ($Q = 1.703$ Å$^{-1}$) and vanishes at $D_2$ fillings beyond $\rho_{D_2} = 0.1$, whereas the high-$Q$ component shifts in position indicating a compression of the layer and increases in height with growing $D_2$ fillings. This behavior points to a coexistence of two phases and is characteristic for a first-order C-IC transition of the Kr film as Nielsen *et al.*[13] have previously observed at much higher temperatures ($T = 40$ K). Here we find the same feature at 1.5 K. At $\rho_{D_2} = 0.20$ a new small Bragg peak emerges at $Q = 2.05$ Å$^{-1}$ which is difficult to see in this diffractogram, but becomes clearly discernible at higher $D_2$ fillings (see Figs. 10 and 11). We interpret this small peak as being caused by some $D_2$-rich islands, which penetrated into the Kr layer and produced the 2D spreading pressure by which the C-IC transition of the Kr layer was induced. This scenario is illustrated schematically in Fig. 2(c). It is evident that small $D_2$ clusters form in the Kr layer and compress it into an incommensurate phase, before the film grows in a layer-on-layer mode. Thus, the simple picture [Fig. 2(b)] inferred from the adsorption

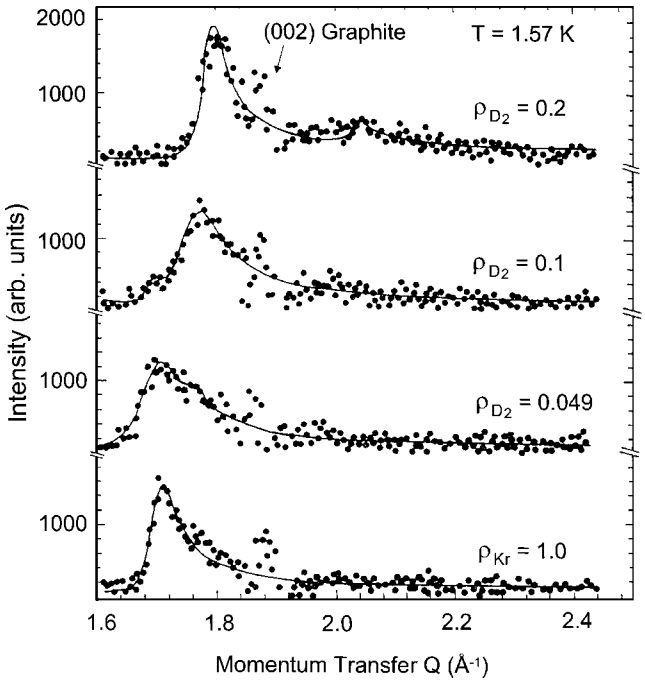


FIG. 9. Neutron-diffraction scans showing the commensurate-incommensurate transition of a preadsorbed complete Kr layer ($\rho_{Kr}=1$) on graphite induced by coadsorption of small doses of $D_2$ ($0.049<\rho_{D_2}<0.2$) at $T=1.57$ K. The C-IC transition of the Kr layer at this low temperature turns out to be first order, because the composite line profile contains Bragg peaks at the *C* and IC positions indicating phase coexistence. The small peak at $Q \approx 2.05$ Å$^{-1}$ arises from $D_2$ clusters within the Kr layer. Solid lines represent powder-averaged 2D Lorentzian-squared line shape fits convoluted with the instrumental resolution to the data.

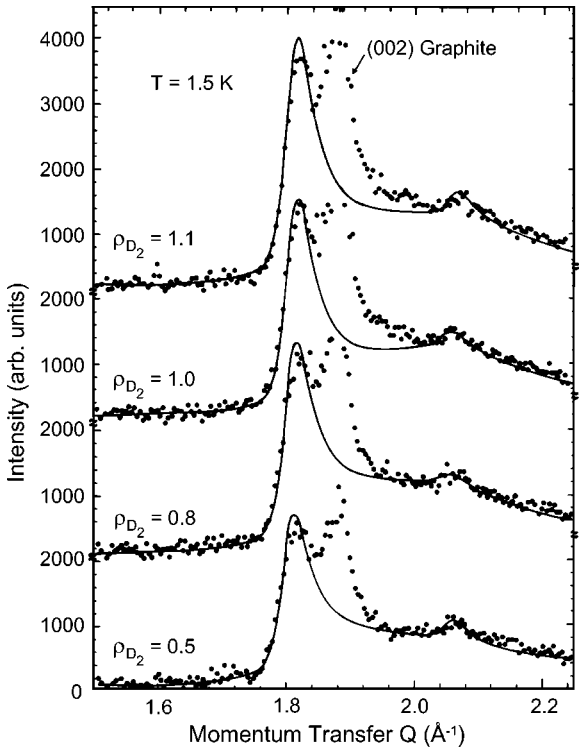


FIG. 10. Series of neutron-diffraction profiles at $T=1.5$ K and various $D_2$ fillings $\rho_{D_2}$ on graphite preplated by a complete Kr layer ($\rho_{Kr}=1$). With growing $D_2$ fillings, the intensity of the principal Bragg reflection increases. As the $D_2$ and Kr reflections coincide, it was concluded that $D_2$ adopts a commensurate $(1\times1)[\frac{1}{2}]$ structure on top of the Kr layer and thus represents a 2D Ising system [see Fig. 1(b)]. The small peaks at $Q\approx2.05$ Å$^{-1}$ are attributed to solid $D_2$ clusters in the Kr layer. Solid lines represent composite line shape fits to the data as described in the text (see Sec. V).

isotherm measurements (Sec. III) has to be revised slightly. Nielsen *et al.*[13] drew the same conclusion, but because they employed x-ray diffraction, they could only see the reaction of the Kr layer. Neutron diffraction has the great advantage that the effects of both coadsorbate components can be explored simultaneously, since the coherent neutron-scattering cross sections differ only by a factor of 3 [$\sigma_{coh}(Kr)=7.67$ b, $\sigma_{coh}(D_2)=22.37$ b].[6]

Figure 10 displays neutron diffractograms at $D_2$ fillings between 0.5 and 1.1 ML at $T=1.5$ K. It is evident that the principle peak at $Q\approx1.8$ Å$^{-1}$ only shifts slightly in position with growing $D_2$ filling, but increases in height. This is due to the fact that the peak positions of both coadsorbate components coincide and leads to the conclusion that $D_2$ adopts a commensurate $(1\times1)[\frac{1}{2}]$ solid phase on top of the incommensurate (IC) Kr spacer layer. Thus, these results give direct evidence that $D_2$ on Kr/graphite forms the expected 2D Ising system over a broad coverage range as indicated in the phase diagram (Fig. 6). As mentioned above, the peak around $Q\approx2.05$ Å$^{-1}$ arises from small $D_2$ clusters within the Kr layer.

Neutron diffraction also allows studying the order-disorder transition of the commensurate $D_2$ layer. Figure 11 presents as examples a few typical diffraction patterns at $D_2$ fillings of $\rho_{D_2}=1.10$ ML (low-temperature value before desorption sets in) and various temperatures. The data clearly exhibit two Bragg reflections at $Q=1.814$ and 2.065 Å$^{-1}$. The main peak results from the combined diffraction effect of 1 ML Kr+1 ML $D_2$. As the temperature rises, the peak height decreases, while the peak positions remain fixed demonstrating that $D_2$ stays registered on the Kr layer until the $D_2$ layer melts at about 25 K. Above this temperature only the Bragg peak of the Kr layer remains, which expands with increasing temperature due to the release of spreading pressure by the desorbing $D_2$ layer (see Fig. 4). A detailed analysis of the intensity of the $D_2$ peak in dependence on temperature will follow in Sec. VI A.

The small peaks at $Q=2.065$ Å$^{-1}$ are again caused by the $D_2$-rich clusters within the Kr layer. It is visible that desorption of part of the $D_2$ layer with increasing temperature leads to a disappearance of these signals. A second reason for their disappearance is melting of the $D_2$ clusters. Assuming an equilaterally spaced triangular IC structure of these clusters, from the peak position $Q=2.065$ Å$^{-1}$ a coverage $\rho=1.48$ or an area density of $n=0.0944$ Å$^{-2}$ can be deduced from the known data of $D_2$ on bare graphite.[5,6] These values are close to those of the densest monolayer of $D_2$ on graphite ($\rho=1.55$ and $n=0.099$ Å$^{-2}$).[6] From the phase diagram of $D_2$/graphite[4,6,25] one can infer that at this coverage the $D_2$ layer melts at about 28 K, which agrees well with our findings that above this temperature the diffraction signals from

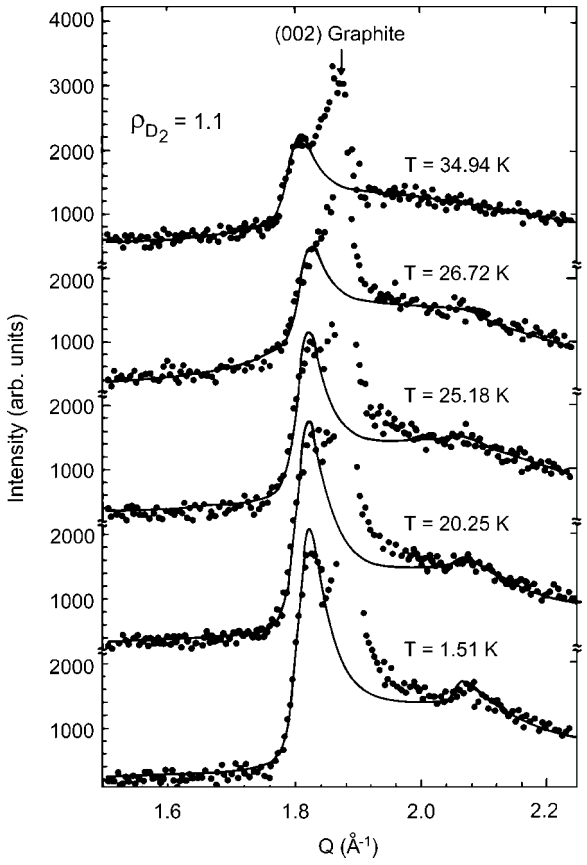


FIG. 11. Evolution of diffraction patterns with temperature for 1.1 ML of $D_2$ (low-temperature value before desorption sets in) on Kr preplated graphite ($\rho_{Kr}=1$). It can be concluded from these data that $D_2$ remains registered on the IC Kr spacer layer before melting at about 25 K. Desorption of $D_2$ above 25 K leads to an expansion of the Kr film and evaporation of the penetrated 2D $D_2$ clusters as can be seen from the spectrum taken at $T=34.94$ K. Solid lines represent composite line shape fits to the data as described in the text (see Sec. V).

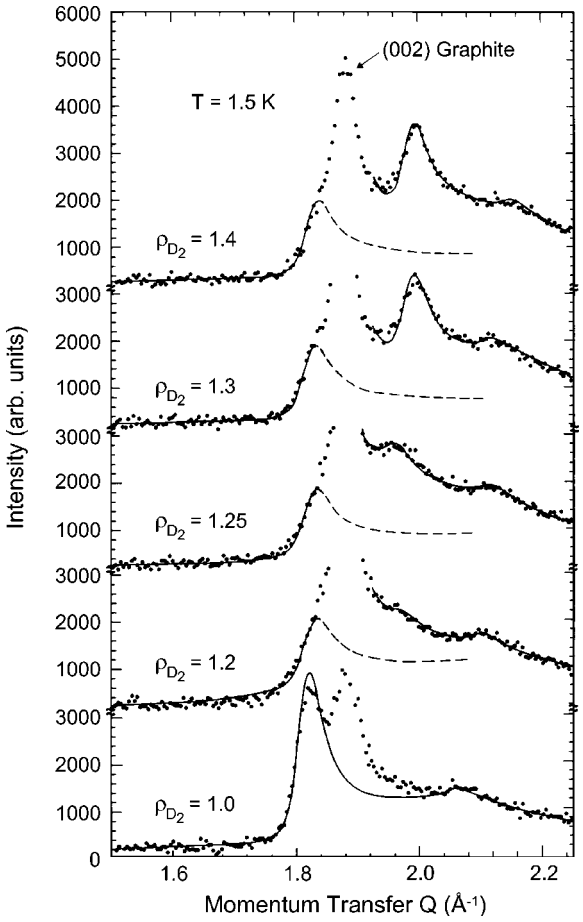


FIG. 12. The evolution of neutron-diffraction profiles of $D_2$ on Kr/graphite when passing through the C-IC transition at $T=1.5$ K (background scattering is subtracted). At $\rho_{D_2}=1.2$ the Bragg peak of the registered $(1\times1)[\frac{1}{2}]$ structure of the $D_2$ layer at $Q=1.82$ Å$^{-1}$ vanishes and only the reflection of the compressed Kr layer is left over indicated by the dashed line. For $1.20<\rho_{D_2}<1.25$ small "liquidlike" signals appear at $Q=1.95$ Å$^{-1}$ which are attributed to the existence of a reentrant fluid phase between the $C$ and IC phases. The $D_2$ layer solidifies again for $\rho\geqslant1.3$ as indicated by pronounced Bragg peaks at $Q\approx1.99$ Å$^{-1}$. The small peaks in the range $2.05\leqslant Q\leqslant2.14$ Å$^{-1}$ arise from $D_2$ clusters within the Kr spacer layer, which are continuously compressed with growing $D_2$ filling. Solid lines represent composite line shape fits to the data as described in the text (see Sec. V).

the 2D $D_2$ clusters within the Kr layer disappeared (see Fig. 11). This observation yields a good cross check that the assignment of the small peaks to 2D $D_2$ clusters is correct.

At coverages beyond $\rho_{D_2}=1.2$, the $D_2$ layer undergoes a commensurate-incommensurate (C-IC) transition (see Fig. 6). Figure 12 shows the evolution of neutron-diffraction patterns across this transition with increasing $D_2$ fillings at $T=1.5$ K. At $\rho_{D_2}=1$ the $D_2$ layer is commensurate on the Kr layer and the Bragg reflections of both layers coincide. For coverages of 1.2 ML $D_2$ and beyond the C-IC transition occurs leading to a strong reduction the intensity of the common layer signal at $Q=1.82$ Å$^{-1}$ to that of the pure Kr spacer layer indicated by the dashed line. First signals of the IC phase appear at $Q\approx1.95$ Å$^{-1}$. They are tiny and broad and have a "liquidlike" shape. In the coverage range $1.20<\rho_{D_2}<1.25$ they remain at the same position $Q$. From the 2D line shape fits (solid lines) to the data, a coherence length of about 30 Å can be extracted. These results strongly support the occurrence of a reentrant fluid phase (domain-wall fluid) at the C-IC transition down to temperatures of 1.5 K in agreement with the heat capacity and entropy data (see Figs. 4, 6, and 7). This is the lowest temperature to which a "liquidlike" phase of $D_2$ has ever been observed.

Increasing the $D_2$ filling further, results in a resolidification of the $D_2$ layer into an equilaterally spaced triangular IC phase as indicated by well-defined Bragg peaks appearing at $\rho_{D_2}=1.30$. As more molecules are incorporated in the layer with growing $D_2$ fillings, the IC solid is uniformly compressed. We did not extend our neutron diffraction studies in sufficient detail to be able to clarify the structures of the various modifications of the IC phase (IC1, IC2, $\kappa$ and $\zeta$ phases), which were found by the methods applied (heat capacity, neutron diffraction) and mapped out in the phase diagram (Fig. 6). It turned out that the $D_2$ layer is complete at $\rho_{D_2}\approx1.55$ (note that this is the same coverage as for $D_2$ on

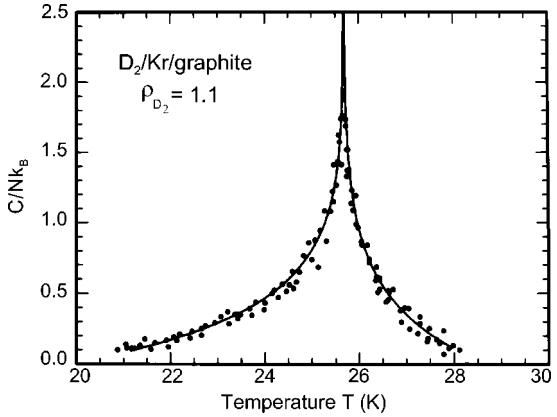


FIG. 13. Heat capacity peak of $D_2$/Kr/graphite at critical $D_2$ filling $\rho_{D_2}=1.10$ ($N$=number of adsorbed $D_2$ molecules, $k_B$ =Boltzmann constant). The background is subtracted from the data. The solid line indicates a nonlinear least-squares fit of the theoretically predicted 2D Ising behavior according to Eq. (2) to the data with a critical temperature $T_c=25.68\pm0.05$ K.

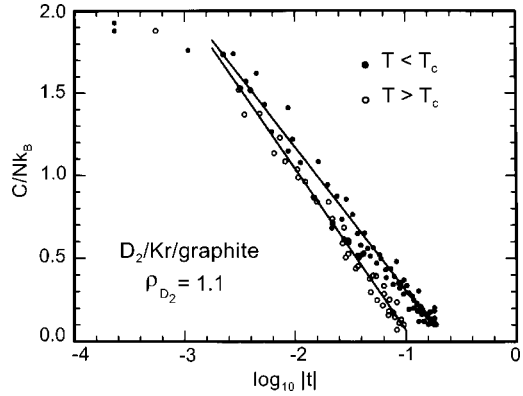


FIG. 14. Semilogarithmic plot of the heat capacity data of Fig. 13 versus the reduced temperature $t=(T-T_c)/T_c$ with $T_c=25.68$ K. The data are well fitted by a logarithmic dependence (solid lines) above and below $T_c$, which is consistent with the 2D Ising model. Differences in the slopes of the straight lines may be an artifact due to uncertainties in background subtraction.

bare graphite[4–6,25]). Beyond this coverage a second $D_2$ layer is built up, which solidifies above $\rho_{D_2}=1.7$ as indicated by the occurrence of an additional Bragg peak at $Q=2.08$ Å$^{-1}$ [see Fig. 19(a)].

The solid lines in Figs. 10–12 represent composite line shape fits to the data. They were obtained by superposition of several contributions: The diffraction peaks of the Kr and the $D_2$ layers, diffraction peaks of $D_2$-rich islands within the Kr spacer layer (all described by powder-averaged Lorentzian-squared line shapes convoluted with instrumental resolution), and a broad Gaussian-shaped background centered between $Q\approx2.02-2.11$ Å$^{-1}$ depending on temperature and coverage. The latter contribution arises when the $D_2$ layer is built up and may be caused by disordered ranges of the film or by stacking faults. It is responsible for the fact (see Fig. 12) that there is an effect in intensity at $Q$ values above the graphite peak. A similar effect has previously been observed in multilayer growth of $D_2$ (Ref. 37) or $N_2$.[40] Since the diffraction contribution of the Kr layer due to compression with increasing $D_2$ filling could not be subtracted from the data, it had an effect on the size and shape of the (002) graphite reflection. Because of the complicated composition of the film, we did not try to fit the data using line shapes modified to include the structure factor of a bi- or trilayer with different stacking sequences.[41,42]

## VI. ANALYSIS OF PHASE TRANSITIONS

In order to be able to classify the system of $D_2$ adsorbed on graphite precoated with an incommensurate monolayer of Kr as a 2D Ising system, we investigated the phase transitions in more detail.

### A. The order-disorder transition at the critical point

First, we will consider the order-disorder transition of the registered $(1\times1)\left[\frac{1}{2}\right]$ phase at the critical point. Figure 13 displays the highest heat capacity peak found at a $D_2$ filling of $\rho_{D_2}=1.10$. Since the Kr layer is compressed due to the penetration of $D_2$ clusters as we have seen in Sec. V, the highest peak appears at a filling, which is 10% greater than that of the complete $\sqrt{3}$ monolayer. The background contribution of the sample cell and the substrate (graphite foam) as well as the contribution due to desorption of the film and a regular part containing all nonsingular contributions of both coadsorbate layers were subtracted from the data. A λ-shaped peak remains, which strongly suggests the occurrence of a continuous phase transition. If it is Ising-like with a critical exponent $\alpha=0$, it should be described by a logarithmic dependence on the reduced temperature $t$ (Refs. 43 and 44) defined as $t=(T-T_c)/T_c$:

$$C_{\pm}=A_{\pm}\ln|t|+B_{\pm}. \tag{2}$$

$T_c$ is the critical temperature and $A_{\pm}$ and $B_{\pm}$ are the critical parameters. The $\pm$ signs refer to the sign of $t$. The solid line in Fig. 13 represents the best fit of this relation to the experimental data with $T_c=25.68\pm0.05$ K. Within experimental scattering, it describes the data very well. This is also evident from a scaling plot (Fig. 14), where the heat capacity data are plotted as a function of the decadic logarithm of the reduced temperature $t$. The data vary approximately linearly with $\log_{10}|t|$ above and below $T_c$ over a range of about two decades in $t$. The rounding close to $T_c(t<10^{-3})$ is caused by finite-size effects (see, e.g., Refs. 45 and 46), because the correlation length of fluctuations is limited by the size of the graphite crystallites. From the fits of the straight lines (solid lines) to the data, the following values of the critical amplitudes were obtained: $A_+=0.42\pm0.01$ for $T>T_c$ and $A_-=0.37\pm0.01$ for $T<T_c$. The critical amplitude ratio $A_+/A_-=1.13\pm0.05$ deviates slightly from its universal value 1, which may be a consequence of uncertainties in the background subtraction. The linear dependence provides evidence that the transition belongs to the 2D Ising universality class.

2D Ising behavior in the neighborhood of the critical point can also be inferred from the temperature dependence of the peak intensities, which were determined from the line

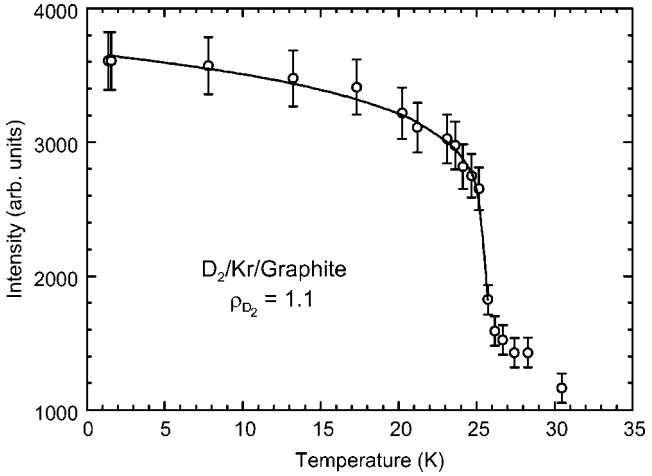


FIG. 15. Plot of maximum peak intensity versus temperature obtained from neutron diffraction spectra (see Fig. 11) of a complete commensurate $(1\times1)\left[\frac{1}{2}\right]$ layer of $D_2$ ($\rho_{D_2}=1.10$) adsorbed on Kr-plated graphite (Papyex). The solid line shows the fit of the 2D Ising model $I\propto|t|^{\beta}$ with $T_c=25.7\pm0.6$ K and critical exponent $\beta=0.12\pm0.02$.

shape fits to the neutron spectra, a few examples of which are shown in Fig. 11. A plot of the maximum peak intensity versus temperature again at the critical $D_2$ filling of 1.10 ML is depicted in Fig. 15. The intensity decays as $T$ increases. However, it does not drop to zero above $T_c$, because the Bragg reflections of the $D_2$ layer are superimposed on those of the Kr spacer layer, which remains solid above the transition. The data were fitted by the power law $I\propto|t|^{\beta}$, where $\beta$ is the critical exponent of the order parameter. The result of the fit is indicated by the solid line and yields a critical exponent of $\beta=0.12\pm0.02$ which is in reasonable agreement with the 2D Ising exponent $\beta=1/8$.[6,7,47] From the fit a critical temperature of $T_c=25.7\pm0.6$ K was determined which is consistent with the more precise calorimetric results.

### B. The order-disorder transition at the tricritical point

A further point of evidence for 2D Ising criticality of the system $D_2/Kr/$graphite is provided by the behavior of the heat capacity in the neighborhood of the tricritical point. At this point the line of continuous transitions of the pure commensurate phase merges into the coexistence line between the $C$ phase and the 2D gas phase (see Fig. 6). In order to characterize the phase transition at this point, a constant coverage heat capacity scan was taken at $\rho_{D_2}=0.91$. The result is presented in Fig. 16. The background of the sample cell including the substrate (graphite foam) was again subtracted. In addition, the data were reduced by the desorption heat capacity and by some nonsingular lattice contributions of the $D_2$-Kr coadsorbate. A single well-defined peak was found, which was fitted by the power law

$$\frac{C_{\pm}}{Nk_B}=A_{\pm}|t|^{\alpha_{\pm}} \tag{3}$$

with the same definition of the critical parameters as in Eq. (2). The reduced temperature $t=(T-T_{TC})/T_{TC}$ is now related

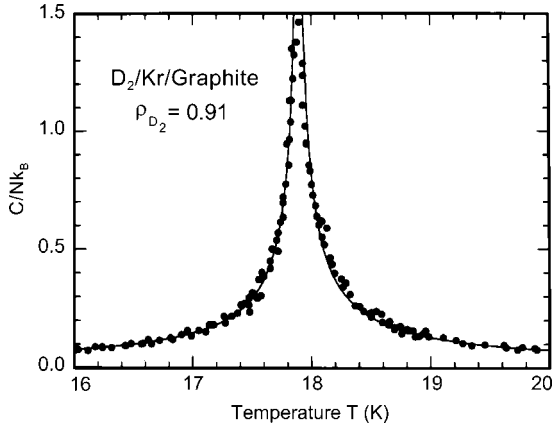


FIG. 16. Heat capacity of $D_2$ on Kr-plated graphite (foam) close to the tricritical point ($N$=number of adsorbed $D_2$ molecules, $k_B$=Boltzmann constant). The $D_2$ filling is 0.91 ML. The nonsingular background contribution is subtracted from the data. The solid line is the result of a nonlinear least-squares fit of Eq. (3) to the data with tricritical point located at $T_{TC}=17.88\pm0.06$ K.

to the temperature of the tricritical point $T_{TC}$. The nonlinear fit to the data (solid lines) yields a tricritical temperature of $T_{TC}=17.88\pm0.06$ K. The critical behavior becomes apparent in a double-logarithmic plot of the data (Fig. 17). They show a linear behavior above and below $T_{TC}$. From the slopes of the straight lines fitted to the data (solid lines), the following values of the tricritical exponents have been extracted:

$$\alpha_+=0.875\pm0.05 \text{ for } T>T_{TC}$$

and

$$\alpha_-=0.870\pm0.05 \text{ for } T<T_{TC}.$$

These values are in excellent agreement with the theoretically predicted value of the tricritical exponent of $\alpha_+=\alpha_-=8/9=0.889$ of the 2D Ising model.[6,7,47–49] To our knowl-

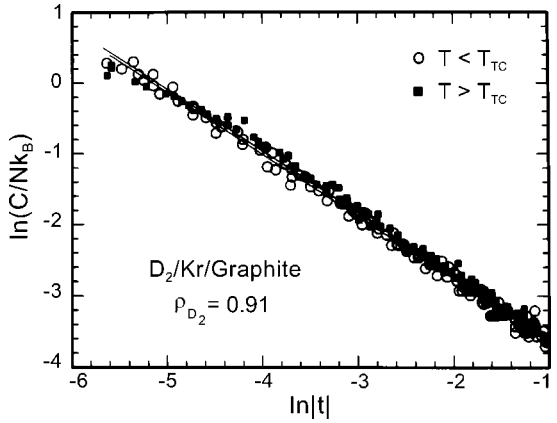


FIG. 17. Log-log plot of the heat capacity data from Fig. 16 versus reduced temperature $t=(T-T_{TC})/T_{TC}$ with $T_{TC}=17.88$ K. Within measurement uncertainties, the slopes of the straight lines fitted to the data correspond to the theoretically predicted value (Refs. 6, 7, and 47–49) of $\alpha=8/9=0.889$ for $T<T_{TC}$ and $T>T_{TC}$.

edge this is the first time that the tricritical exponent for a 2D Ising system could be experimentally determined in adsorbates.

### C. The commensurate-incommensurate transition

Another fascinating phenomenon, which has never been investigated before, is the commensurate-incommensurate (C-IC) transition of a 2D Ising system. According to the theory[16,17,50–53] a dramatic difference should occur compared to the C-IC transition of a 2D three-state Potts system.[4–6,54,55] This difference is rationalized in the Kosterlitz-Thouless[17–19,56] criterion

$$p^2 > 8 \tag{4}$$

which characterizes the stability of a slightly incommensurate phase. This means that the type of the phase diagram at the C-IC transition depends crucially on the number of energetically equivalent adsorption sites $p$. For $p=3$, the three-state Potts model, condition (4) is fulfilled and the theory[16,17] predicts a direct second-order transition from the C to the IC solid phase. However, if the dislocation core energy is low, the presence of bound dislocation pairs at moderately high temperatures may cause the elastic constants of the domain-wall lattice to be small so that a dip in the fluid phase boundary near the C-IC transition may occur. Halpin-Healy and Kardar[52] applied the striped helical Potts model[57,58] and found that a solid striped domain-wall (SIC) phase may be squeezed in between the $C$ and IC phases. This case is sketched in Fig. 18(a). This type of phase diagram was also experimentally observed for the isotopic molecular hydrogens $H_2$ and HD (Refs. 4, 6, and 59–62) and for $^3$He and $^4$He on bare graphite.[63,64] For $D_2$/graphite the C-IC transition turned out to be more complicated because here the striped phase gives way to a hexagonal heavy domain-wall structure before entering into the IC phase.[4–6,25,65,66] The phase diagrams of the 2D quantum systems could be verified by computer simulations.[33,34]

For the 2D Ising system with $p=2$ the situation changes dramatically. Now the Kosterlitz-Thouless criterion (4) is not fulfilled any more and the striped domain-wall phase (SIC) is unstable to the spontaneous formation of free dislocations, cannot sustain shear and thus should be a liquidlike phase [reentrant fluid (RF), domain-wall fluid]. This leads to the prediction of the schematic phase diagram depicted in Fig. 18(b). The reentrant fluid (RF) phase should intervene between the $C$ and the IC phases down to absolute zero.[16,17]

What happens in reality for the 2D Ising system $D_2$/Kr/graphite? We have already learned from the results of the volumetric, calorimetric and entropy measurements (see Secs. III and IV) that a disordered or liquidlike wedge extends down to at least 1.5 K. This was also mapped out in the phase diagram (Fig. 6). The neutron-diffraction profiles exhibited liquidlike line shapes at $D_2$ fillings between 1.20 and 1.25 ML (see Fig. 12). This is also reflected in Figs. 19(a) and 19(b), where the positions of all Bragg peaks and peak intensities are plotted versus the $D_2$ filling $\rho_{D_2}$ at 1.5 and 4.5 K. The $Q$ values and intensities were determined from line shape fits to the diffraction profiles (Figs. 9, 10, and 12).

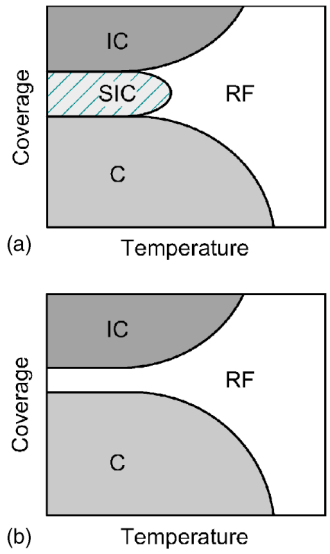


FIG. 18. Sketches of two possible generic phase diagrams in the neighborhood of the commensurate-incommensurate (C-IC) transition for (a) a three-state Potts system ($p=3$) and (b) a 2D Ising system ($p=2$). In case (a) the transition may proceed via solid domain-wall phases, e.g., a striped domain-wall phase (SIC), and in case (b) via a reentrant fluid (RF) phase (Refs. 16 and 17). The SIC phase is expected to be melted by a small but growing population of wall crossings (Ref. 52) as the temperature is raised. The RF phase is regarded as a domain-wall fluid consisting of a tangled, incoherent array of domain-wall segments and crossings diffusing around. According to the Kosterlitz-Thouless criterion (4) for the 2D Ising model, this phase should extend down to $T=0$ K between the $C$ and IC phases.

The dashed and dotted lines separate the different phase regions found which are marked by letters A–F and correspond to the identical regions in the phase diagram (Fig. 6). At small doses of $D_2$ the transition from the commensurate $(\sqrt{3}\times\sqrt{3})R30°$ phase of the Kr spacer layer to an IC phase is induced as concluded from Fig. 9. At $D_2$ fillings between $0.2<\rho_{D_2}<1.2$ we have the broad coexistence range between gas and the registered $(1\times1)\left[\frac{1}{2}\right]$ phase on the Kr layer which leads to an almost constant $Q$ value (only very modest compression of the $D_2$ layer), but a linear increase of intensity, because more and more 2D patches of the $(1\times1)\left[\frac{1}{2}\right]$ phase are built up. Unfortunately, the hatched $Q$ range in Fig. 19(a) is inaccessible to neutron diffraction due to the overlap with the strong graphite (002) reflection. The C-IC transition of the $D_2$ layer takes place beyond $\rho_{D_2}=1.2$, which causes a drastic change of the film properties. The diffraction signal jumps to a new position of $Q=1.95$ Å$^{-1}$ and the intensity drops dramatically because of the combined effects of separation of the $D_2$ and Kr peaks and because of the liquidlike character of the reentrant fluid (see Fig. 12). It is remarkable that the peak positions stay constant in the small region $1.20<\rho_{D_2}<1.25$ and that the intensities do not vary very much, which is a further convincing evidence for the existence of the reentrant fluid phase. Beyond $\rho_{D_2}=1.25$ the peaks shift again and their intensity increases due to a resolidification of the layer in an IC phase. It is uniformly compressed as more molecules are incorporated in the layer. The

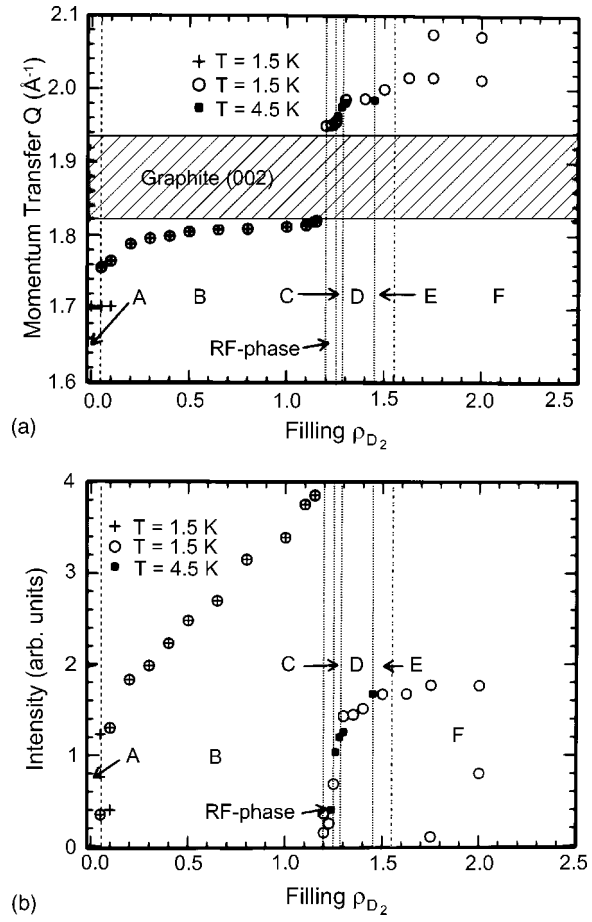


FIG. 19. (a) Neutron-diffraction peak positions $Q$ versus $D_2$ filling $\rho_{D_2}$ on Kr preplated graphite at 1.5 K (open circles) and 4.5 K (solid squares). The crosses mark the Kr peak positions, the dashed and dotted lines the coverage ranges of the various phases corresponding to the phase diagram (Fig. 6), the double-dotted-dashed line the completion of the first $D_2$ layer. Note that the $D_2$ peak position levels off in the RF phase. (b) Maximum neutron-diffraction peak intensity versus $D_2$ filling at the same temperatures as in (a). The dramatic intensity drop at $\rho_{D_2}=1.2$ is caused by the C-IC transition and reflects that the Kr and $D_2$ peaks separate and that the $D_2$ film enters the reentrant fluid phase. According to the present measurements, it extends at least down to 1.5 K. Nomenclature (see Fig. 6 for comparison). A: Commensurate $(\sqrt{3}\times\sqrt{3})R30°$ structure of Kr/graphite, B: Commensurate $(1\times1)[\frac{1}{2}]$ structure of $D_2$ on IC Kr/graphite, RF: Reentrant fluid phase of $D_2$/Kr/graphite, C: First incommensurate $D_2$ phase (IC1), D: $\kappa$ phase, E: Second incommensurate $D_2$ phase (IC2), F: Bilayer structure of $D_2$/Kr/graphite.

$D_2$ layer is complete at $\rho_{D_2}=1.55$ as inferred from the constancy of peak position and intensity. Beyond this coverage, the second layer is built up. The second Bragg peak arising above $\rho_{D_2}=1.7$ indicates the solidification of the $D_2$ bilayer.

The present studies provide experimental evidence that the C-IC transition of a 2D Ising system is in fact a melting transition as predicted by the theory of Coppersmith *et al.*[16,17] They also verify the validity of the Kosterlitz-Thouless criterion [see Eq. (4)]. Experimental hints for the liquidlike character of the reentrant fluid phase for HD adsorbed on Kr preplated graphite, a system with a presumably similar phase diagram, was obtained from quasielastic neutron-scattering (QENS) measurements.[67] Recently, for HD adsorbed on bare graphite the liquidlike nature of the reentrant fluid phase could be directly proven by high-resolution QENS experiments.[68]

## VII. CONCLUSIONS AND SUMMARY

In the present studies volumetric adsorption isotherm, calorimetric and neutron diffraction measurements were employed to explore the phase diagram of $D_2$ physisorbed on an incommensurate monolayer of Kr on graphite. The experimental conditions were controlled by adsorption isotherm measurements, which exhibited a layer-on-layer (LL) growth mode at least up to the formation of the third $D_2$ layer. Though occurring in a much smaller coverage range than for $D_2$/graphite, a substep in an adsorption isotherm for $D_2$/Kr/graphite was attributed to a commensurate-incommensurate transition in the $D_2$ film. The results of the thermodynamic measurements (adsorption isotherms, heat capacity temperature scans, and heat capacity isotherms) allowed constructing the phase diagram of $D_2$ adsorbed on graphite preplated by a monolayer of Kr ($\rho_{Kr}=1$) up to the coverage of a compressed $D_2$ layer. The dominant feature of the phase diagram is a broad coexistence range between a commensurate ($C$) phase and 2D gas at $D_2$ fillings below $\rho_{D_2}=1.2$ and temperatures below 17.9 K. The pure commensurate phase only exists in a small coverage range at low temperatures and its range broadens due to thermal contributions at high temperatures. The $C$ phase melts at $T_c=25.68$ K at the critical point. Compared to $D_2$ on bare graphite ($T_c=18.1$ K) this is an unusually high temperature, which seems to be caused by the high potential corrugation of the Kr layer. Interestingly, from desorption peaks determined by heat capacity measurements a binding energy of the $D_2$ molecules to the Kr layer was estimated which is by a factor of 3 smaller than that of $D_2$ on bare graphite. The larger distance of the $D_2$ layer to the graphite substrate, in combination with the effect of the Kr layer, obviously leads to the reduction of the holding potential.

The structure of the $C$ phase was determined by neutron diffraction experiments, which revealed that adsorbing $D_2$ on top of the Kr spacer layer compresses this layer to an incommensurate phase. It could be shown that a small fraction ($\approx10\%$) of the $D_2$ molecules penetrate into the Kr layer and form small 2D islands. The resulting enhanced spreading pressure of the film induces a first-order C-IC transition of the Kr film at 1.5 K as has previously been found out by Nielsen *et al.*[13] at much higher temperatures ($T=40$ K). Beyond $\rho_{D_2}\approx0.2$, the $D_2$ molecules are ordered in patches of the commensurate $(1\times1)[\frac{1}{2}]$ structure on top of the IC Kr spacer layer. With growing $D_2$ filling, the number of these patches increases in coexistence with 2D gas until the total Kr layer is covered by the $D_2$ film. Entropy determinations revealed that the $D_2$ film is in a state of disorder in the coverage range $1.20<\rho_{D_2}<1.25$ and at temperatures down to at least 1.5 K. This gap in the phase diagram was attrib-

uted to the existence of a reentrant fluid phase, a conclusion, which could be directly demonstrated by the neutron diffraction measurements. At higher coverages ($\rho_{D_2} > 1.25$), the $D_2$ film orders in an incommensurate structure. Due to the quantum nature of the $D_2$ film, it turned out to be highly compressible until monolayer completion is reached at about $\rho_{D_2} = 1.55$. Beyond this coverage the second $D_2$ layer is formed.

The most interesting feature of the phase diagram is the existence of a commensurate $(1\times1)[\frac{1}{2}]$ phase. It exhibits 2D Ising symmetry. In order to show this unambiguously, three phase transitions were investigated in detail.

(a) The order-disorder transition of the complete commensurate $(1\times1)[\frac{1}{2}]$ structure at the critical point ($T_c = 25.68$ K, $\rho_{D_2} = 1.10$).

(b) The order-disorder transition at the tricritical point ($T_{TC} = 17.88$ K, $\rho_{D_2} = 0.91$).

(c) The commensurate-incommensurate transition occurring beyond $\rho_{D_2} = 1.2$.

The analysis of all the data provides clear evidence for a 2D Ising behavior. The critical exponents of the heat capacity and the order parameter at the critical point and of the heat capacity at the tricritical point were determined and good agreement with theoretical predictions was obtained. The critical behavior of a 2D Ising system realized by an adsorbed system near the tricritical point has never been investigated before. Also the C-IC transition of a 2D Ising system could be studied. It was observed that at this transition a reentrant fluid phase (domain-wall fluid) squeezes in between the C and IC phases down to temperatures of 1.5 K in a small coverage range. This is the lowest temperature to which a liquidlike phase of $D_2$ has ever been detected. The observation of this phase unambiguously confirms the Kosterlitz-Thouless criterion[16–19,56] and the theory of the C-IC transition,[16,17,50–53] which in turn verifies the 2D Ising character of this system. The results of these experiments have clearly demonstrated that the quantum coadsorbate $D_2/Kr/$graphite is a new model system, which can be classified as a 2D Ising system.

## ACKNOWLEDGMENTS

This research work has been financially supported by the BMBF (Bundesministerium für Bildung und Forschung, Grant No. 03-WI3Mai-4), by the DFG (Deutsche Forschungsgemeinschaft, Collaborative Research Center 262), and by the Materials Science Research Center (MSRC, Mainz, Germany). H.W. and K.-D.K. wish to thank the Hahn-Meitner-Institut (BENSC), Berlin, Germany, for hospitality during the neutron diffraction measurements.

[1] J.G. Dash, Phys. Rep., Phys. Lett. **38C**, 177 (1978).
[2] M. Bretz, Phys. Rev. Lett. **38**, 501 (1977).
[3] M. Bretz, J.G. Dash, D.C. Hickernell, E.O. McLean, and O.E. Vilches, Phys. Rev. A **8**, 1589 (1973).
[4] H. Wiechert, Physica B **169**, 144 (1991).
[5] H. Freimuth, H. Wiechert, H.P. Schildberg, and H.J. Lauter, Phys. Rev. B **42**, 587 (1990).
[6] H. Wiechert, *Adsorption of Molecular Hydrogen Isotopes on Graphite and Boron Nitride*, in Landolt-Börnstein New Series III/42-A3, Physics of Covered Solid Surfaces, Chapter 3.6.2, edited by H.P. Bonzel (Springer-Verlag, Berlin, 2003), p. 166.
[7] F.Y. Wu, Rev. Mod. Phys. **54**, 235 (1982).
[8] M.J. Tejwani, O. Ferreira, and O.E. Vilches, Phys. Rev. Lett. **44**, 152 (1980).
[9] E. Domany, M. Schick, J.S. Walker, and R. B. Griffiths, Phys. Rev. B **18**, 2209 (1978).
[10] E. Domany and M. Schick, Phys. Rev. B **20**, 3828 (1979).
[11] M. Schick, in *Phase Transitions in Surface Films I*, edited by J.G. Dash and J. Ruvalds (Plenum Press, New York, 1980), p. 65.
[12] M. Schick, Prog. Surf. Sci. **11**, 245 (1981).
[13] M. Nielsen, J. Als-Nielsen, J. Bohr, and J.P. McTague, Phys. Rev. Lett. **47**, 582 (1981).
[14] H. Wiechert, K.-D. Kortmann, and N. Stüßer, Physica B **234–236**, 164 (1997).
[15] H. Wiechert and K.-D. Kortmann, J. Low Temp. Phys. **111**, 561 (1998).
[16] S.N. Coppersmith, D.S. Fisher, B.I. Halperin, P.A. Lee, and W.F. Brinkman, Phys. Rev. Lett. **46**, 549 (1981).
[17] S.N. Coppersmith, D.S. Fisher, B.I. Halperin, P.A. Lee, and W.F. Brinkman, Phys. Rev. B **25**, 349 (1982).
[18] J.M. Kosterlitz and D.J. Thouless, in *Progress in Low Temperature Physics*, Vol. VII b, edited by D.F. Brewer (North-Holland, Amsterdam, 1978), p. 371.
[19] J.M. Kosterlitz and D.J. Thouless, J. Phys. C **6**, 1181 (1973).
[20] H. Wiechert and K.-D. Kortmann, Surf. Sci. **441**, 65 (1999).
[21] R.J. Birgeneau, P.A. Heiney, and J.P. Pelz, Physica B **109-110**, 1785 (1982).
[22] D. Marx and H. Wiechert, in *Surface Properties, Vol. 95 of Advances in Chemical Physics*, edited by I. Prigogine and St. A. Rice (Wiley, New York, 1996), p. 213.
[23] H. Asada, S. Doi, and H. Kawano, Surf. Sci. Lett. **273**, L 403 (1992).
[24] F.-Ch. Liu, Y.-M. Liu, and O.E. Vilches, Surf. Sci. **294**, 265 (1993).
[25] H. Freimuth and H. Wiechert, Surf. Sci. **178**, 716 (1986).
[26] K.-D. Kortmann, Ph.D. Thesis, Johannes Gutenberg-University, Mainz, 1997.
[27] P.S. Ebey, Y.-M. Liu, and O.E. Vilches, J. Low Temp. Phys. **100**, 131 (1995).
[28] L. Mattera, F. Rosatelli, C. Salvo, F. Tommasini, U. Valbusa, and G. Vidali, Surf. Sci. **93**, 515 (1980).
[29] J.G. Dash, *Films on Solid Surfaces* (Academic Press, New York, 1975).
[30] G.A. Stewart and J.G. Dash, Phys. Rev. A **2**, 918 (1970).
[31] A.D. Novaco and F.J. Milford, Phys. Rev. A **5**, 783 (1972).
[32] S.B. Crary and O.E. Vilches, Phys. Rev. Lett. **38**, 973 (1977).
[33] E. Vives and P.-A. Lindgård, Surf. Sci. Lett. **284**, L449 (1993).
[34] E. Vives and P.-A. Lindgård, Phys. Rev. B **47**, 7431 (1993).

[35] M. Kreer and P. Nielaba, in *Monte Carlo and Molecular Dynamics of Condensed Matter Systems*, edited by K. Binder and G. Cicotti (Societa Italiana di Fisica, Bologna, 1996), p. 501.
[36] P. Nielaba, in *Frontiers in Materials Modelling and Design*, edited by V. Kumar, S. Sengupta, and B. Raj (Springer-Verlag, Berlin, 1998), p. 325.
[37] H. Wiechert, in *Excitations in Two-Dimensional and Three-Dimensional Quantum Fluids*, edited by A.F. G. Wyatt and H.J. Lauter (Plenum Press, New York, 1991), p. 499.
[38] B.E. Warren, Phys. Rev. **59**, 693 (1941).
[39] H.P. Schildberg and H.J. Lauter, Surf. Sci. **208**, 507 (1989).
[40] S.-K. Wang, J.C. Newton, R. Wang, H. Taub, J.R. Dennison, and H. Shechter, Phys. Rev. B **39**, 10 331 (1989).
[41] J.Z. Larese, M. Harada, L. Passell, J. Krim, and S. Satija, Phys. Rev. B **37**, 4735 (1988).
[42] J.Z. Larese, Q.M. Zhang, L. Passell, J.M. Hastings, J.R. Dennison, and H. Taub, Phys. Rev. B **40**, 4271 (1989).
[43] L. Onsager, Phys. Rev. **65**, 117 (1944).
[44] B.M. McCoy and T.T. Wu, *The Two-Dimensional Ising Model* (Harvard University Press, Cambridge, MA, 1973).
[45] V. Privman, *Finite Size Scaling and Numerical Simulation of Statistical Systems* (World Scientific, Singapore, 1990).
[46] K. Binder, Rep. Prog. Phys. **60**, 487 (1997).
[47] A. Patrykiejew, S. Sokołowski, and K. Binder, Surf. Sci. Rep. **37**, 207 (2000).
[48] R.B. Pearson, Phys. Rev. B **22**, 2579 (1980).
[49] B. Nienhuis, J. Phys. A **15**, 199 (1982).
[50] P. Bak, Rep. Prog. Phys. **45**, 587 (1982).
[51] See, e.g., M. den Nijs, in *Phase Transitions and Critical Phenomena*, edited by C. Domb and J.L. Lebowitz (Academic Press, London, 1988), Vol. 12, p. 219.
[52] T. Halpin-Healy and M. Kardar, Phys. Rev. B **34**, 318 (1986).
[53] B.N.J. Persson, Surf. Sci. Rep. **15**, 1 (1992).
[54] P.W. Stephens, P.A. Heiney, R.J. Birgeneau, P.M. Horn, D.E. Moncton, and G.S. Brown, Phys. Rev. B **29**, 3512 (1984).
[55] E.D. Specht, A. Mak, C. Peters, M. Sutton, R.J. Birgeneau, K.L. D'Amico, D.E. Moncton, S.E. Nagler, and P.M. Horn, Z. Phys. B: Condens. Matter **69**, 347 (1987).
[56] H.J. Schulz, Phys. Rev. B **22**, 5274 (1980).
[57] M. Kardar and A.N. Berker, Phys. Rev. Lett. **48**, 1552 (1982).
[58] T. Halpin-Healy and M. Kardar, Phys. Rev. B **31**, 1664 (1985).
[59] H. Wiechert and H. Freimuth, in *Proceedings of the 17th International Conference on Low Temperature Physics LT-17*, edited by U. Eckern, A. Schmid, W. Weber, and H. Wühl (North-Holland, Amsterdam, 1984), p. 1015.
[60] H. Freimuth and H. Wiechert, Surf. Sci. **162**, 432 (1985).
[61] H. Wiechert, H. Freimuth, and H.J. Lauter, Surf. Sci. **269/270**, 452 (1992).
[62] H. Freimuth, H. Wiechert, and H.J. Lauter, Surf. Sci. **189/190**, 548 (1987).
[63] S.V. Hering, S.W. van Sciver, and O.E. Vilches, J. Low Temp. Phys. **25**, 793 (1976).
[64] D.S. Greywall, Phys. Rev. B **47**, 309 (1993).
[65] J. Cui, S.C. Fain, Jr., H. Freimuth, H. Wiechert, H.P. Schildberg, and H.J. Lauter, Phys. Rev. Lett. **60**, 1848 (1988).
[66] J. Cui and S.C. Fain, Jr., Phys. Rev. B **39**, 8628 (1989).
[67] H. Wiechert, K.-D. Kortmann, M. Bienfait, and R. Kahn (unpublished).
[68] H. Wiechert, B. Leinböck, M. Bienfait, and M. Johnson, Physica B **329–333**, 426 (2003).